Aluminium foam/steel interface formed during foaming process in air or argon flow: a micro structural comparison.

Monno M.[a,b], Mussi V.[a], Negri D.[a]
[a] *Laboratorio MUSP,Piacenza, Italy*
[b] *Politecnico di Milano – Dipartimento di Meccanica*

1. Introduction

Metal foams are characterised by a cellular structure which gives them high energy absorption and damping capacities. Light aluminium metal foams have been thus proposed as filling reinforcement materials in hollow structures, for example to improve impact behaviour in protection systems in automotive field, or as vibration damper in machine tools. In order to improve the behaviour of hollow structures, a metallurgical bonding at the interface should allow the foam filling to be firmly fixed to the internal walls of the structure giving it bending and torsional strength higher than those of the starting component.

The formation of an intermetallic layer when solid iron comes in contact with molten aluminium is typical of several technological processes. Diffusion of Fe and Al atoms leads to the formation and growth of the intermetallic layer trough a process that is initially reaction diffusion and then follows parabolic kinetics during its growth [1, 2, 3, 4, 5]. The properties of the intermetallic layer depend on the type, morphologies and thicknesses of the phases formed. Many research works studied the role of alloying elements in the composition of the steel and aluminium melt (C, Si, Fe, Mn, Ti and Ni) [6, 7, 8, 9] and the thickness and morphology of the intermetallic layers to improve tensile strength, elongation and ductility, neutralising the brittleness of AlFeSi intermetallics for aluminium melt in contact with solid metal. The formation and characterisation of the intermetallic phases formed at the interface between the metal foam and steel [10,11] and their role on the mechanical properties has not been clarified up to now. The formation of the metallurgical bonding seems to be hampered by the short contact time between the solid metal and the molten aluminium during the foaming process and by the oxidation of both the foam and the internal mould's surface during the expansion [10]. Aim of this work was to compare the composition and the microstructure of the interface layer between a foam from a commercial PM precursor and a low carbon steel plate during foaming in air or in inert atmosphere constraining the foam expansion.

2. Experimental

Commercial foamable precursors of two different compositions: AlSi10 (0.8 wt.% TiH_2 as blowing agent), very close to the eutectic composition and AlMg1Si0.6 (0.8 wt.% TiH_2), to minimise the negative effect of silicon in wetting between Al and Fe, have been foamed on a S355J2 low carbon steel (0.188 wt% C) plate. Precursor specimens (15 x 10 x 4.5 mm) were

positioned on the steel substrate (ϕ: 56 mm, thickness 4.5 mm) and foamed for 10 min in a convection heating furnace pre heated at 700 ^{o}C. Precursors' and substrates' surfaces were mechanically smoothed and cleaned to obtain a uniform heat transfer during heating and to reduce the oxidation effects. Foaming tests were performed both in air and in flowing argon. The thermal history of the specimens was followed by two thermocouples (K type) positioned directly into the specimen and under the sample holder (Figure 1). From preliminary tests it was realised that constraining the foam expansion prevents the argon or air to stir up the sample in the first instants when the foam expands upward thus maximizing the contact (both time and surface) between foam and solid thus improving the formation of metallurgical bonding. In subsequent experiments precursor pieces were arranged in the closed equipment sketched in Figure 1. Argon gas flushes from two lateral holes in order to uniformly wrap the precursor tablet.

Foamed specimens were cut perpendicular to the substrate/foam interface and prepared for microstructural examinations of the interlayer between foam and substrate. The as prepared cross sections have been observed by both optical and scanning electron microscopy. Letiz Aristomet metallographic microscope underlined the formation of metallurgical bonding at the foam/substrate interface. ZEIS EVO 50 XVP Scanning electron microscope (resolution: 3 nm for secondary electron and 4.5 nm for back scattered electron) coupled with an INCA ENERGY 200 dispersive X-ray (EDS) system was used to distinguish the different phases present in the layer and to try to propose a possible phase identification trough its elemental composition. The specimens' surfaces were gold coated to prevent charging effects. The identification of phases was also verified by X-ray diffraction measurements (XRD). Specimens for diffraction analysis were sectioned parallel to the substrate/foam interface. Foam was polished out to remove step wise Al until the intermetallic layer was reached. Diffractograms were collected using Cu-Kα radiation in the range of $5^{o} \leq 2 \leq 70^{o}$, with a step size of 0.02^{o} and a counting time of 4 s per step using a Brucker diffractometer. Microhardness measurements were performed on the same sections already analysed by electron microscopy to further clarify the intermetallic layers. Vickers microhardness tester LEIKA VMHT30A (load: 1, 10 g for intermetallic layers and matrix and substrate respectively, t= 15 s) has been used. Indentation positions were chosen on a grid at a distance of 10 μm one from each other so as to eliminate effects of neighbouring indentation (spot size of the order of 1 – 2 μm). Samples were successively observed by backscattered electrons in order to identify the belonging layer of each spot. The diagonals of the indentations were measured using ImageJ software [12] for image analysis and used to calculate the Vicker's hardness value.

3. Results and discussion

The thermocouple inserted in the precursor's billet allowed to record the temperature evolution during the foaming process (Figure 2). The changes in the curvature of the heating curve at temperature around 578 ^{o}C and 655 ^{o}C were representative of the fusion process in AlSi10 and AlMg1Si0.6 precursors respectively while those on the cooling curve underlined the solidification of the foamed samples in air outside the furnace.

SEM images (Figure 3) highlighted the interface between foam and substrate: the aluminium foam could be easily distinguished from the iron substrate and the intermetallic layer between them could also be evidenced. It was possible to observe that when the foaming

happened in argon flux a continuum and uniform bonding layer formed between foam and substrate while for air foamed specimens the intermetallic layer appeared only in a limited zone, probably corresponding to those small areas where there was a real contact between precursor and steel.

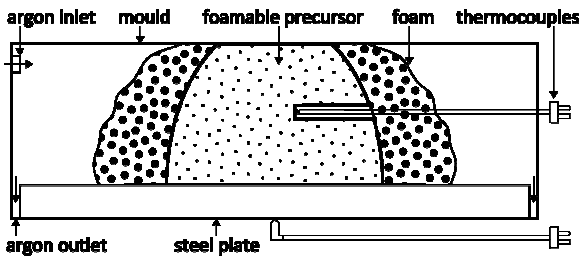

Figure 1. Schematic draw of the equipment used for foaming.

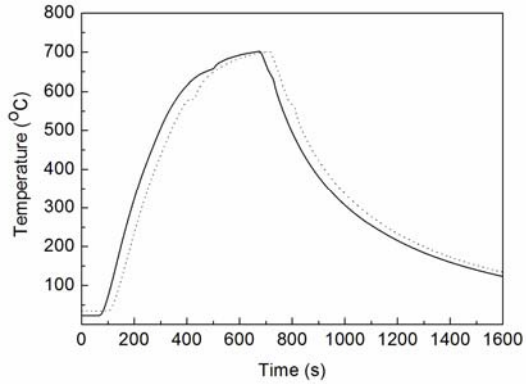

Figure 2. Temperature evolution for AlSi10 (dotted line) and AlMg1Si0.6 (solid line) precursors during foaming on the low carbon steel plate.

As it can be assumed that any intermetallic phase, generated during the foaming process, was the result of the contact between the liquid foam and the solid steel, it was reasonable to observe a quite continuum but thinner layer for AlMg1Si0.6 precursor and a rather fragmented one for the precursor containing more Si (Figure 3d) [13].

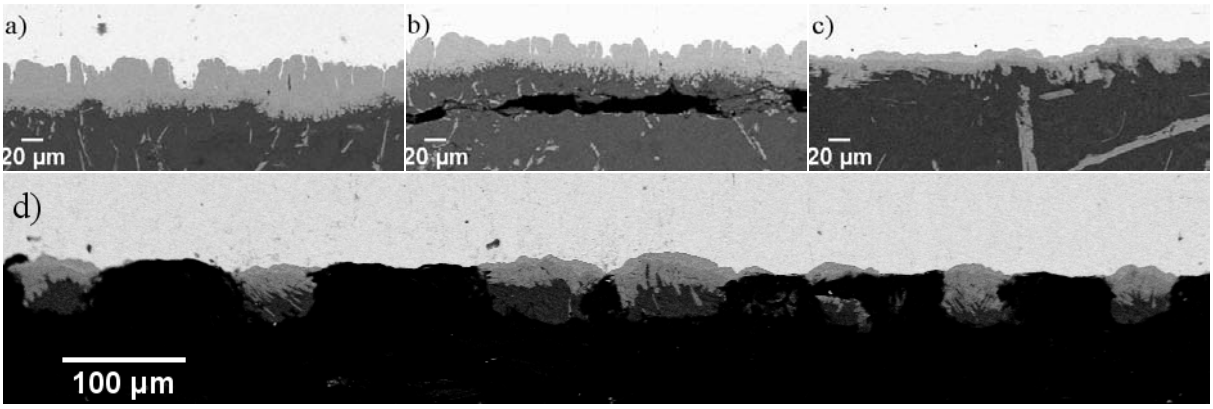

Figure 3. Scanning electron micrographs (BSE signal) of the interface between foam and steel substrate:
a) AlMg1Si0.6 foamed in Argon b) AlMg1Si0.6 foamed in air c) AlSi10 foamed in Ar, d) AlSi10 foamed in air.

Backscattered SEM images at higher magnification reported in Figure 4 clearly showed the formation of a two phase layer for AlMg1Si0.6 precursors foamed both in air and in argon flux, while a threefold layer was observed for AlSi10 precursors foamed in air and in Ar. The similarity of the layers, belonging to precursors of the same composition, foamed in air and in argon was not only morphological but also compositional. The elemental percentages detected by electron probe microanalysis measurements in different positions at the interface (Table 1) suggested the identification of the intermetallic phases. The clearer layer about 20 µm thick, marked by A, richer in iron and closer to the steel substrate, was characterized by a

composition which is in the stability range of existence of orthorhombic Fe_2Al_5 phase. It showed the serrated tongue-like shape typical of Fe_2Al_5 phase formed in dipping experiments between pure iron and pure aluminium [1, 2, 3]. The darker and thinner layer (about 12 µm), labelled B, closer to aluminium foam, could be identified as the minor phase $FeAl_3$ formed between solid iron and molten aluminium. The aluminium side of this layer showed a blocky structure, characterised by darker regions within it with texture and shade similar to that of Al alloy, that could be ascribed to aluminium that remains liquid during the formation of the intermetallic phase. The interface of AlSi10 specimen evidenced the formation of three intermetallic layers about 8 µm thick each. While A and B layers are quite continuous the C one appeared interrupted. The SEM – EDX results (Table 1) indicated a strong influence of silicon in the formation of the intermetallic phases between foam and low carbon steel substrate. Moving from aluminium foam to the substrate a β – $Al_{4.5}FeSi$ phase, also known as $_6$, followed by an α – Al_8Fe_2Si phase, also known as $_5$, typical of rich Al corner in the AlFeSi phase diagram were identified, while a $Fe_2(Al,Si)_5$ phase, characterised by a composition similar to that of Fe_2Al_5 intermetallic layer, observed for AlMg1Si0.6 precursor, was observed close to iron.

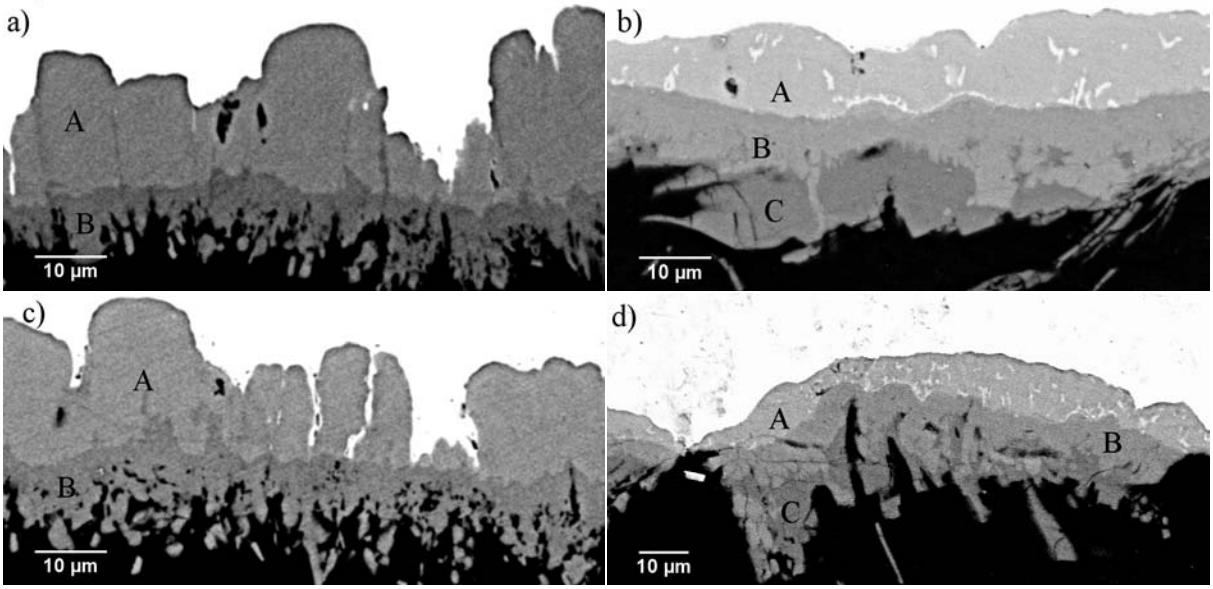

Figure 4. Scanning electron micrographs of the interface between foam and steel substrate: a) AlMg1Si0.6 foamed in argon, b) AlSi10 foamed in Argon, c) AlMg1Si0.6 foamed in air, d) AlSi10 foamed in air.

AlMg1Si0.6		*O*	*Al*	*Si*	*Mn*	*Fe*	*AlSi10*		*O*	*Al*	*Si*	*Mn*	*Fe*
air	A	1.58	54.86	1.20	0.67	41.69	Air	A	2.25	52.53	1.64	0.76	42.81
	B	1.70	59.50	1.29	0.47	37.04		B	1.92	53.80	11.29	0.39	32.60
								C	2.10	54.22	16.46	0.39	26.83
argon	A	1.59	54.23	0.89	0.57	42.72	argon	A	1.58	51.52	3.40	0.49	43.01
	B	1.79	59.36	0.63	0.40	37.81		B	2.05	54.44	11.16	0.42	31.93
								C	1.94	55.19	15.91	0.09	26.87

Table 1. Elemental composition (wt%) in positions indicated by capital letters in Figure 4.

Intermetallic layers close to the substrate in specimens belonging from precursors rich in Si, foamed both in Ar and in air, were characterised by brighter spots both at the interface with the intermetallic and dispersed in the matrix. EDX line profile presented in Figure 5 showed an increase in Si concentration and a decrease an Al concentration across the brighter spots

while the percentages of iron (43.8 wt.%), silicon (1.7 wt.%) and aluminium (53.6 wt.%) in the matrix (indicated with B in Figure 5a) quite agreed with the values reported Fe_2Al_5.

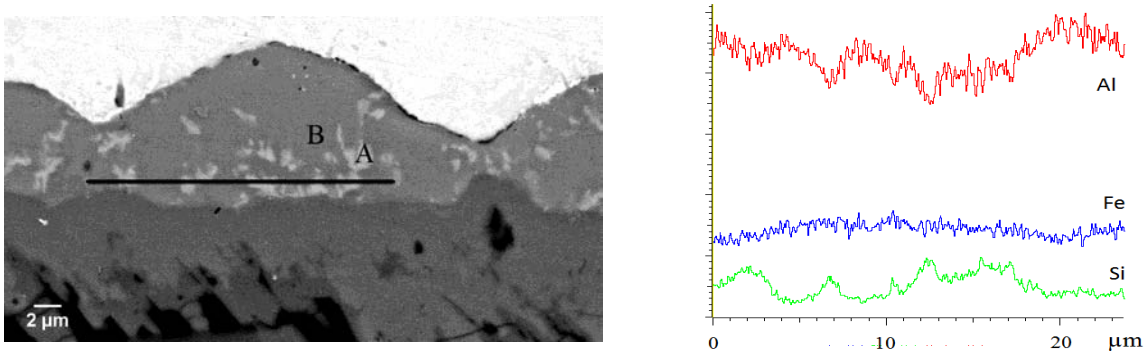

Figure 5. Electron probe microanalysis line profile crossing several bright spot: a) SEM micrograph, b) variation of the elemental concentration.

AlSi10	*HV*	*Sample std. dev*	*Number of indentations*	*AlMg1Si0.6*	*HV*	*Sample std. dev*	*Number of Indentations*
A	608.94	87.93	16	A	520.35	57.08	17
B	529.04	77.74	10	B	413.61	34.78	9
C	387.15		6				

Table 2. Vicker's hardness values of indentations in intermetallic layer of different composition at the interface between foam and steel substrate for AlSi10 and AlMg1Si0.6 precursors.

Microhardness tests were performed across the interface intermetallic layer to evaluate the mechanical properties of the various constituents present in the microstructure. The mean Vicker's hardness values are reported in Table 2 for each layer. Statistical analysis of the results allowed to distinguish three layers of different hardness for AlSi10 precursor and two layers for AlMg1Si0.6. Three and two phases of increasing hardness could be distinguished going from foam to steel substrate for AlSi10 and AlMg1Si0.6 precursors respectively. These results suggested the importance of elemental diffusion from the steel substrate in the molten aluminium matrix (foam).

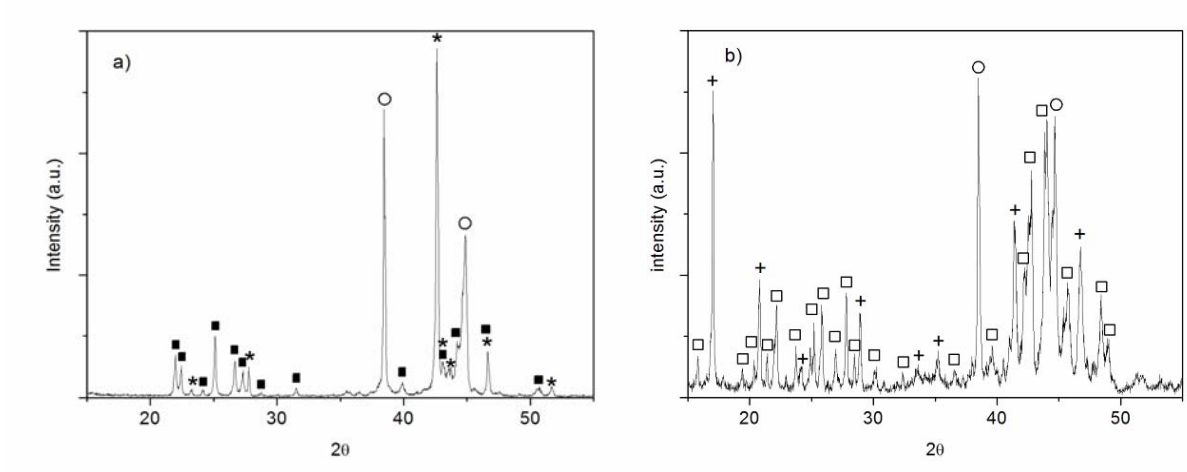

Figure 6. X ray diffraction patterns of the intermetallic layer at the foam/steel interface in specimens foamed from: a) AlMg1Si0.6 precursor showing the presence of Al ( ), $FeAl_3$ (■) and Fe_2Al_5 (*); b) AlSi10 precursor showing the presence of Al ( ), Fe_2Al_8Si (+) and FeAl5Si.

X ray diffraction patterns of the intermetallic layer formed by AlMg1Si0.6 and AlSi10 precursors foamed in argon atmosphere showed typical reflections corresponding to Al, $FeAl_3$, Fe_2Al_5 (Figure 6a) and Al, Fe_2Al_8Si (α phase) and $FeAl_5Si$ (β phase) (Figure 6b) respectively. The simultaneous presence of different phases in the two samples was due to the irregular shape of the intermetallic layers as is evident from Figure 4. Electron probe microanalysis on the XRD analysed surfaces confirmed the presence of areas with different elemental compositions in agreement with the range of stability of the phases identified in XRD patterns.

4. Conclusions

A detailed microstructural characterisation of the intermetallic layer at the foam/substrate interface showed a uniform and continuous layer formed when the foaming process was performed in argon flux even for silicon rich precursor. An almost continuous layer was observed for AlMgSi0.6 foam foamed in air but the foam detached from the substrate during sectioning while the intermetallic layer remained with it. For AlSi10 precursor the intermetallic layer was observed only in correspondence of pits on the steel surface where its formation seams to start. A double layer was observed for low silicon precursor showing the presence of Fe_2Al_5 near steel and $FeAl_3$ close to Al foam. A three phase layer characterised the intermetalic layer formed by the precursor with high Si percentage. Going from the foam to the substrate: β ($FeAl_5Si$), α (Fe_2Al_8Si) and $Fe_2(Al,Si)_5$ could be identified. The morphology and composition of the formed intermetallic layer did not change for foaming in air or in Ar. Though the major elements found in the intermetallic layers are the same i.e. Al, Fe and Si the morphological and mechanical properties of the phases formed are the result of the different percentages of these elements underlying the importance of elemental interdiffusion in the process of bonding between foam and substrate.

5. Acknowledgment

The research has been carried out in the frame of the research project INTEMA funded by the Italian Ministry of Research under the “PRIN” program. The authors would like to express their gratitude to Dr L. Zampori of the Dipartimento di Chimica, Materiali e Ingegneria Chimica “G. Natta” - Politecnico di Milano, for his important contribution to the X ray diffraction in this work.

6. References

1 H. R. Shaverdi, M.R. Ghomashchi, S. Shabestari, J. Hejazi, J. Mater. Sci. 2002, 37, 1061 – 1066.
2 K. Bouchè, F. Barbier, A. Coulet, *Mat.Sci.Eng. A* 1998, 249, 167 - 165
3 A.Bouayad, Ch. Gerometta, A. Bekebir, A. Ambari, Mat. Sci. Eng. A 2003, 363, 53 – 61.
4 V. I. Dybkov, J. Mater. Sci. 1986, 21, 3085 – 3090.

5 V.I. Dybkov, J. Mater. Sci. 1986, 21, 3078 – 3084.
6 Sung-Ha Hwang, Jin-Hwa Song, Yong-Suk Kim, Mat. Sci. Eng. A 2005, 390, 437 – 443.
7 T. Sasaki, T. Yakou, K. Mochiduki, K. Ichinose, ISIJ International 2005, 45, 1887 – 1892.
8 K.A. Nazari, S.G. Shabestari, J. Alloys and Compounds 2009, 478, 523 – 530
9 S.H. Shabestari, Mat. Sci. Eng. A 2004, 383, 289 – 298
10 L. Bonaccorsi, E. Proverbio, N. Raffaele, J. Mater. Sci. 2010, 45, 1514 – 1522.
11 L. Vendra, A. Rabiei, Mat. Sci. Eng. A 2007, 465, 59 – 67.
12 W.S. Rasband, ImageJ, U. S. National Institutes of Health, Bethesda, Maryland, USA, http://rsb.info.nih.gov/ij/, 1997-2005.
13 W.Fragner, B. Zberg, R. Sonnleitner, P. Uggowitzer, J. Loffler, Mat.Sci.Forum 2006, 519 – 521, 1157-1162